Reentrant phase behavior in active colloids with attraction

Gabriel S. Redner, Aparna Baskaran, and Michael F. Hagan*
Martin Fisher School of Physics, Brandeis University, Waltham, Massachusetts, USA
(Received 19 April 2013; published 26 July 2013)

Motivated by recent experiments, we study a system of self-propelled colloids that experience short-range attractive interactions and are confined to a surface. Using simulations we find that the phase behavior for such a system is reentrant as a function of activity: phase-separated states exist in both the low- and high-activity regimes, with a homogeneous active fluid in between. To understand the physical origins of reentrance, we develop a kinetic model for the system's steady-state dynamics whose solution captures the main features of the phase behavior. We also describe the varied kinetics of phase separation, which range from the familiar nucleation and growth of clusters to the complex coarsening of active particle gels.

DOI: 10.1103/PhysRevE.88.012305 PACS number(s): 64.75.Xc, 47.63.Gd, 87.18.Hf

I. INTRODUCTION

The collective behaviors of swarming organisms such as birds, fish, insects, and bacteria have long been subjects of wonder and fascination, as well as scientific study [1]. From a physicist's perspective, such systems can be understood as fluids driven far from equilibrium by the injection of kinetic energy at the scale of individual particles, leading to a zoo of unusual phenomena such as dynamical self-regulation [2], clustering [3–8], segregation [9], anomalous density fluctuations [10], and strange rheological and phase behavior [11–15]. Recently, nonliving systems that also exhibit collective behaviors have been constructed from chemically propelled particles undergoing self-diffusophoresis [16–19], squirming droplets [20], Janus particles undergoing thermophoresis [21,22], and vibrated monolayers of granular particles [23–25], suggesting the possibility of creating a new class of active materials with properties not achievable with traditional materials. However, designing such systems is presently hindered by an incomplete understanding of how emergent patterns and dynamics depend on the interplay between activity and microscopic interparticle interactions.

In this work we investigate an apparent conflict between two recently reported effects of activity on the phase behavior of active fluids. We recently studied [6] a system of self-propelled hard spheres (with no attractive interactions) in which activity *induces* a continuous phase transition to a state in which a high density solid coexists with a low density fluid, complete with a binodal coexistence curve and critical point. This athermal phase separation is driven by self-trapping [4,5]. Separately, a study of swimming bacteria with depletion-induced attractive interactions [26] demonstrated that activity *suppresses* phase separation, an effect which those authors postulate is generic.

We resolve this apparent paradox by demonstrating that the phase diagram for a system of particles endowed with both attractive interactions and nonequilibrium self-propulsion is *reentrant* as a function of activity. Depending on parameter values, activity can either compete with interparticle attractions to suppress phase separation or act cooperatively to enhance it. At low activity, the system is phase-separated due to attraction, while moderate activity levels suppress this clustering to produce a homogeneous fluid. Increasing activity even further induces self-trapping, which returns the system to a phase-separated state. We construct a simple kinetic model whose analytic solution captures the form of this unusual phase diagram and explains the mechanism by which activity

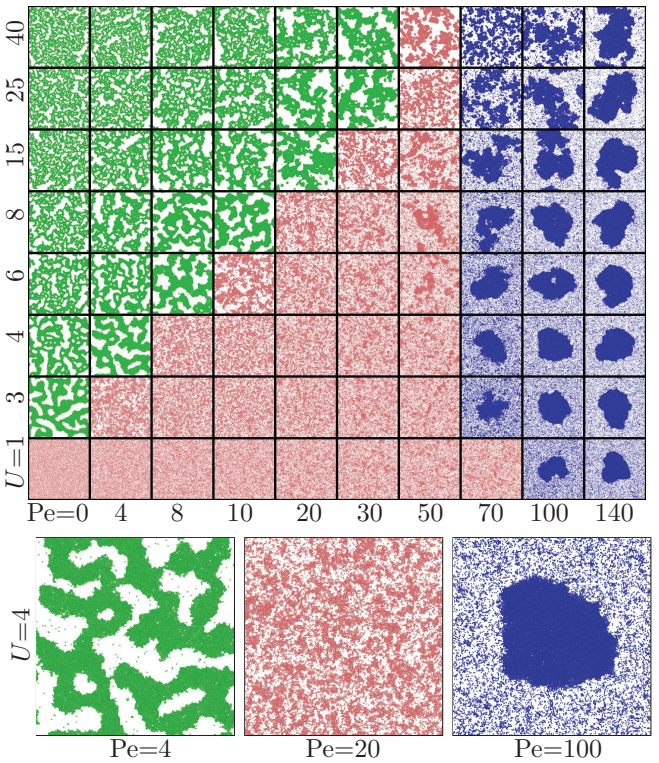

FIG. 1. (Color online) Top: Phase diagram illustrated by simulation snapshots at time $t = 1000\tau$ with area fraction $\phi = 0.4$, as a function of interparticle attraction strength U and propulsion strength Pe. The colors are a guide to the eye distinguishing near-equilibrium gel states (upper-left) from single-phase active fluids (center) and self-trapping-induced phase-separated states (right). Bottom: Detail of reentrant phase behavior at $U = 4$ as Pe is increased. At Pe $= 4$ (left), the system is nearly thermal and forms a kinetically arrested attractive gel. Increasing Pe to 20 (center) suppresses phase separation and produces a homogeneous fluid characterized by transient density fluctuations. Increasing Pe further to 100 (right) results in athermal phase separation induced by self-trapping.

*hagan@brandeis.edu

can both suppress and promote phase separation in different regimes. We also describe the kinetics of phase separation, which differ significantly between the near-equilibrium and high-activity phase-separated states. The behaviors we observe are robust to variations in parameter values, and thus could likely be observed in experimental systems of self-propelled, attractive colloids such as those studied in Refs. [16,26,27].

II. MODEL

Our model is motivated by recently developed experimental systems of self-propelled colloids sedimented at an interface [16,27] and consists of smooth spheres immersed in a solvent and confined to a two-dimensional plane [6]. Each particle is active, propelling itself forward at a constant speed. Since the particles are smooth spheres and we neglect all hydrodynamic coupling [28], they do not interchange angular momentum, and thus there are no systematic torques that might lead to alignment. However, the particles' self-propulsion directions undergo rotational diffusion; based on experimental observations [27], we confine the propulsion directions to be always parallel to the surface. For simplicity, interparticle interactions are modeled by the standard Lennard-Jones potential $V_{\rm LJ} = 4\epsilon\left[\left(\frac{\sigma}{r}\right)^{12} - \left(\frac{\sigma}{r}\right)^{6}\right]$, which provides hard-core repulsion as well as short-range attraction, with σ the nominal particle diameter, and ϵ the depth of the attractive well.

The state of the system is represented by the positions and self-propulsion directions $\{\boldsymbol{r}_i,\theta_i\}_{i=1}^{N}$ of the particles, and their evolution is governed by the coupled overdamped Langevin equations:

$$\dot{\boldsymbol{r}}_i = \frac{1}{\gamma}\boldsymbol{F}_{\rm LJ}(\{\boldsymbol{r}_i\}) + v_{\rm p}\hat{\boldsymbol{v}}_i + \sqrt{2D}\,\boldsymbol{\eta}_i^{\rm T}, \tag{1}$$

$$\dot{\theta}_i = \sqrt{2D_{\rm r}}\,\eta_i^{\rm R}. \tag{2}$$

Here, $\boldsymbol{F}_{\rm LJ} = -\nabla V_{\rm LJ}$, $v_{\rm p}$ is the magnitude of the self-propulsion velocity, and $\hat{\boldsymbol{v}}_i = (\cos\theta_i, \sin\theta_i)$. The Stokes drag coefficient γ is related to the diffusion constant by the Einstein relation $D = \frac{k_{\rm B}T}{\gamma}$. $D_{\rm r}$ is the rotational diffusion constant, which for a sphere in the low-Reynolds-number regime is $D_{\rm r} = \frac{3D}{\sigma^2}$. The η are Gaussian white noise variables with $\langle\eta_i(t)\rangle = 0$ and $\langle\eta_i(t)\eta_j(t')\rangle = \delta_{ij}\delta(t-t')$.

We nondimensionalized the equations of motion using σ and $k_{\rm B}T$ as basic units of length and energy, and $\tau = \frac{\sigma^2}{D}$ as the unit of time. Our Brownian dynamics simulations employed the stochastic Runge-Kutta method [31] with an adaptive time step, with maximum value $2\times10^{-5}\tau$. The potential $V_{\rm LJ}$ was cut off and shifted at $r = 2.5\sigma$.

III. PHASE BEHAVIOR

We parametrize the system by three dimensionless variables: the area fraction ϕ, the Péclet number ${\rm Pe} = v_{\rm p}\frac{\tau}{\sigma}$, and the strength of attraction $U = \frac{\epsilon}{k_{\rm B}T}$. In order to limit our investigation to regions with nontrivial phase behavior, we fix the area fraction at $\phi = 0.4$. At this density, a passive system (${\rm Pe} = 0$) is supercritical for $U \lesssim 2.2$, and phase-separated for stronger interactions [32]. For purely repulsive self-propelled particles, the system undergoes athermal phase separation as a result of self-trapping for ${\rm Pe} \gtrsim 85$ and remains a homogeneous fluid for smaller Pe [6].

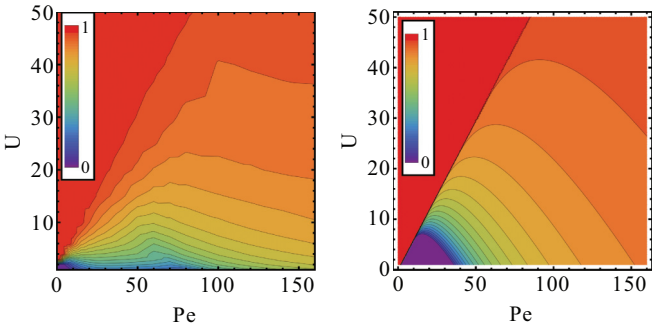

FIG. 2. (Color online) Left: Fraction of particles in clusters $f_{\rm c}$ measured from simulations as a function of Pe and U. Right: $f_{\rm c}$ as predicted by our analytic theory [Eq. (3)], which reproduces the major features of the phase diagram, including the gel region for ${\rm Pe} < U$, the self-trapping region for high Pe, and the low-$f_{\rm c}$ fluid regime in between. The values of the adjustable parameters are $\kappa = 2$ and $f_{\rm max} = 1.7$, with the fit made by eye.

To understand the phase behavior away from these limits, we performed simulations in a periodic box with side length $L = 200$ (with resulting particle count $N = 20\,371$) for a range of attraction strengths $U \in [1,50]$ and propulsion strengths ${\rm Pe} \in [0,160]$. Except where noted, each simulation was run until time 1000τ. Systems were initialized with random particle positions and orientations except that (1) particles were not allowed to overlap and (2) each system initially contained a close-packed hexagonal cluster composed of 1000 particles to overcome any nucleation barriers. To quantify clustering, we consider two particles bonded if their centers are closer than a threshold and identify clusters as bonded sets of more than 200 particles. The cluster fraction $f_{\rm c}$ is then calculated as the total number of particles in clusters divided by N.

The behavior of the system is illustrated in Fig. 1 by representative snapshots (see also S1, S2, and S3 in the Supplemental Material [33]), and in Fig. 2 with a contour plot of $f_{\rm c}$. The most striking result is that the phase diagram is reentrant as a function of Pe. As shown in Fig. 1, low-Pe systems form kinetically arrested gels [34], which gradually coarsen toward bulk phase separation. Increasing Pe to a moderate level destabilizes these aggregates and produces a homogeneous fluid, while increasing activity beyond a second threshold accesses a high-Pe regime in which self-trapping [4–6] restores the system to a phase-separated state.

As evident in Fig. 1, the width of the intermediate single-phase region shrinks as the attraction strength U increases, eliminating reentrance for $U \gtrsim 40$. This trend can be schematically understood as follows. In the low-activity gel states, particles are reversibly bonded by energetic attraction. Particles thus arrested have random orientations, and so the mean effect of self-propulsion is to break bonds and pull aggregates apart. This opposes the influence of attraction, and so the width of the low-Pe gel region increases with U. By contrast, at high Pe we find that self-trapping is the primary driver of aggregation. As shown in the next section, energetic attractions act cooperatively with self-trapping in this regime

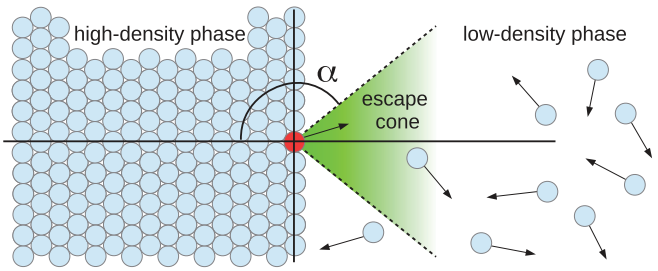

FIG. 3. (Color online) Schematic representation of our kinetic model. The high- and low-density phases fill the left and right half-spaces. A particle on the cluster surface (center) escapes only if its direction points within the "escape cone" defined by $\gamma v_p(\hat{\mathbf{v}} \cdot \hat{\boldsymbol{n}}) > F_{max}$, while particles in the gas land on the surface at a rate proportional to the gas density and propulsion speed.

to enable phase separation at lower Pe than would be possible with activity alone.

IV. KINETIC MODEL

To better understand the physical mechanisms underlying the reentrant phase behavior, we develop a minimal kinetic model to describe the phase separated state. By analytically solving the model, we obtain a form for f_c that captures the major features of the phase behavior observed in our simulations. In the model we consider a single large close-packed cluster coexisting with a dilute gas, which is assumed to be homogeneous and isotropic (Fig. 3). Particles in the cluster interior are assumed to be held stationary in cages formed by their neighbors, but their propulsion directions θ_i continue to evolve diffusively.

To calculate the rate at which gas-phase particles condense onto the cluster, we observe that the flux of gas particles traveling in a direction $\hat{\mathbf{v}}$ through a flat surface is $\frac{1}{2\pi}\rho_g v_p(\hat{\mathbf{v}} \cdot \hat{\boldsymbol{n}})$, with ρ_g the number density of the gas and $\hat{\boldsymbol{n}}$ normal to the surface. Integrating over angles for particles traveling toward the surface of our cluster yields the condensation flux $k_{in} = \frac{\rho_g v_p}{\pi}$.

Next, we estimate the rate of evaporation. We note that a particle on the cluster surface remains bound so long as the component of its effective propulsion force along the outward normal $\gamma v_p(\hat{\mathbf{v}} \cdot \hat{\boldsymbol{n}})$ is less than F_{max}, the maximum restoring force exerted on a particle being pulled away from the surface. This force may involve multiple bonds and is not simply related to the interparticle attraction force. As shown in Fig. 3, this implies an "escape cone" in which the particle's director must point in order for it to escape. The critical angle is $\alpha = \pi - \cos^{-1}\left(\frac{U f_{max}}{\mathrm{Pe}}\right)$, with f_{max} the nondimensionalized maximum restoring force scaled by the depth of the attractive well, which subsumes all relevant details of the binding force and is treated as a fitting parameter: $f_{max} = \frac{F_{max}}{U}\frac{\sigma}{k_B T}$.

We now consider the steady-state angular probability distribution of particles on the cluster surface $P(\theta)$. In the absence of condensation, this distribution evolves according to the diffusion equation with absorbing boundaries at the edges of the escape cone: $\frac{\partial P(\theta,t)}{\partial t} = D_r \frac{\partial^2 P(\theta,t)}{\partial \theta^2}$ and $P(\pm\alpha,t) = 0$, with general solution $P(\theta,t) = \sum_{q=1}^{\infty} A_q \cos\left(\frac{q\pi\theta}{2\alpha}\right) e^{-D_r \frac{q^2\pi^2}{4\alpha^2} t}$. The flux of particles leaving the cluster is then $k_{out} = -\frac{1}{\sigma}\frac{\partial}{\partial t}\int_{-\alpha}^{\alpha} P(\theta,t)d\theta|_{t=0}$. To simplify the analysis, we note that higher-order terms decay rapidly in time, so the steady-state behavior is dominated by the $q = 1$ term. We therefore discard higher-order terms and solve to find $k_{out} = \frac{D_r \pi^2}{4\sigma\alpha^2}$.

From visual observations it is clear that this minimal model does not capture all microscopic details of the interfacial region. In reality, the cluster surface is neither flat nor close packed but has a complex form that is constantly reshaped by fluctuations in both phases (see S4 and S5 in the Supplemental Material [33]). We therefore expect quantitative deviations from the model predictions, which we capture in a general fitting parameter κ that modifies the evaporative flux: $k_{out} = \frac{D_r \pi^2 \kappa}{4\sigma\alpha^2}$.

Equating k_{in} and k_{out} yields a steady-state condition that can be solved for the gas density ρ_g. Since the densities of the two phases are known (the cluster is assumed to be close-packed with density $\rho_c = \frac{2}{\sigma^2\sqrt{3}}$) and the number of particles is fixed, we can calculate the cluster fraction f_c:

$$f_c = \frac{16\phi\alpha^2 \mathrm{Pe} - 3\pi^4\kappa}{16\phi\alpha^2 \mathrm{Pe} - 6\sqrt{3}\pi^3\phi\kappa}. \quad (3)$$

As shown in Fig. 2, this model reproduces the essential features of our system, including active suppression of phase separation at low Pe, activity-induced phase separation at high Pe, and a reentrant phase diagram. The model thus extends the analysis in Ref. [6] to describe the coupled effects of activity and energetic attraction. As noted in that reference, our model description of self-trapping can be considered a limiting case of the theory of Tailleur and Cates [4,5] in which a self-propulsion velocity that decreases with density leads to an instability of the homogeneous initial state.

V. PHASE SEPARATION KINETICS

The kinetics of phase separation differ significantly between the low-Pe gel and high-Pe self-trapping regions. In low-Pe systems, thermal influences dominate and the kinetics are those of a colloidal particle gel [34]. Since the area fraction in our simulations is high, the gels we observe appear nonfractal. Thermal agitation gradually reorganizes the gel into increasingly dense structures [35,36], leading toward a single compact cluster in the infinite-time limit. The presence of activity greatly accelerates the rate at which the gel evolves, as shown in Figs. 4 and 5. This effect is also visible in Fig. 1, as the apparent correlation length in the gel states (each observed after a fixed amount of simulation time) increases with Pe.

As Pe is increased beyond the threshold value $\mathrm{Pe} \approx U$, activity begins to overwhelm energetic attraction and the gel is ripped apart. This arrests the compaction, resulting in a plateau in the system's total potential energy (Fig. 5). Just above this transition, the system resembles a fluid of large mobile clusters, which rapidly split, translate, and merge (Fig. 4). As Pe is further increased, the characteristic mobile cluster size decreases until the appearance of an ordinary active fluid of free particles is recovered. The fluid phase is clearly identified by superdiffusive mean-square displacement measurements (Fig. 5), distinct from the subdiffusive behavior found in gels.

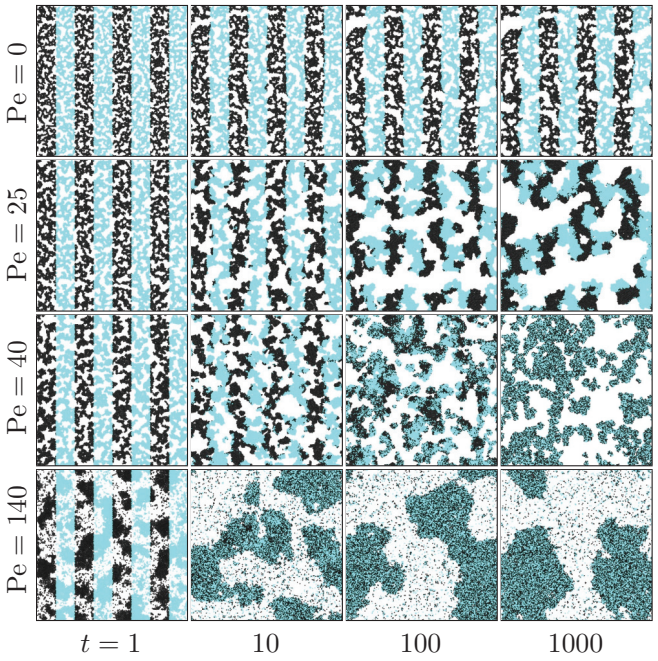

FIG. 4. (Color online) Visual guide to phase-separation kinetics at fixed $U = 30$. To make mixing visible, particles are labeled in two colors based on their positions at $t = 1$. A passive system (top row) forms a space-spanning gel that gradually coarsens. The addition of activity (second row) greatly increases the rate at which the gel evolves. In both cases, particles remain "local" and largely retain the same set of neighbors. When Pe exceeds U (third row), activity is strong enough to break the gel filaments and a fluid of large mobile clusters results. While the instantaneous configurations appear structurally similar to the gels above, these systems quickly become well-mixed due to splitting and merging of clusters (see also Fig. 5). In the high-Pe limit (bottom row), self-trapping drives the emergence of a single well-mixed cluster surrounded by a dilute gas.

Additional increase of Pe will eventually cross a second threshold into a phase-separated regime whose behavior is dominated by self-trapping. As reported previously [6], these systems undergo nucleation, growth, and coarsening stages in a manner familiar from the kinetics of quenched fluid systems, albeit with the unfamiliar control parameter Pe instead of temperature.

These three regimes are characterized by dramatically different particle dynamics. To illustrate these behaviors and their effect on particle reorganization timescales, in Fig. 4 we present snapshots from simulations in which initial particle positions are identified by color. We see that when attraction is dominant ($U >$ Pe), each particle's set of neighbors remains nearly static over the timescales simulated, indicative of long relaxation timescales due to kinetic arrest. In contrast, when activity dominates (Pe $> U$), particles rapidly exchange neighbors and the system becomes well-mixed. Importantly, note that particle dynamics cannot be directly inferred from the instantaneous spatial structures in the system. For example,

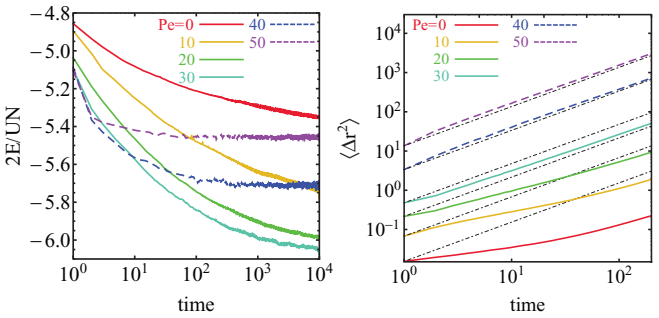

FIG. 5. (Color online) Quantitative measurements of states with $U = 30$. Left: Mean interaction energy per particle (E represents the total system potential energy). Low-Pe gels are strongly arrested and do not approach bulk phase-separation on our simulation timescales; however, higher-Pe systems evolve much faster and nearly reach the bulk limit. When Pe $> U$ (dashed lines), coarsening is arrested as the gel breaks into a fluid of mobile clusters with a Pe-dependent characteristic size, leading to a plateau in the system potential energy. Right: Discrimination of gel from fluid states by mean-square displacement. Dotted lines have slope 1 and highlight the distinction at short times between gels (subdiffusive) and active fluids (superdiffusive).

while systems with low activity (Pe $< U$; Fig. 4, second row) and moderate activity (Pe $\gtrsim U$; Fig. 4, third row) appear structurally similar, the rate of particle mixing differs by orders of magnitude.

VI. CONCLUSIONS

Activity can both suppress and induce phase separation, and we have shown that these opposing effects can coexist in the same simple system. The resulting counterpoint produces a reentrant phase diagram in which two distinct types of phase separation exist, separated by a homogeneous fluid regime. This surprising result makes it possible to use two experimentally accessible control parameters (Pe and U) in concert to tune the phase behavior of active suspensions. This control is especially valuable because attractive interparticle interactions are common in experimental active systems, being either intrinsic [16,27] or easily imposed, such as by the addition of depletants [26]. An understanding of the complex phase behavior accessible to these systems is a critical stepping stone toward designing smart active materials whose phases and structural properties can dynamically respond to conditions around them.

ACKNOWLEDGMENTS

This work was supported by NSF-MRSEC-0820492 (G.S.R., A.B., M.F.H.), as well as NSF-DMR-1149266 (A.B.). Computational support was provided by the National Science Foundation through XSEDE computing resources (Trestles) and the Brandeis HPC.

[1] T. Vicsek and A. Zafeiris, Phys. Rep. **517**, 71 (2012).
[2] A. Gopinath, M. F. Hagan, M. C. Marchetti, and A. Baskaran, Phys. Rev. E **85**, 061903 (2012).
[3] F. Peruani, A. Deutsch, and M. Bär, Phys. Rev. E **74**, 030904 (2006).
[4] J. Tailleur and M. E. Cates, Phys. Rev. Lett. **100**, 218103 (2008).

[5] M. E. Cates and J. Tailleur, EPL (Europhys. Lett.) **101**, 20010 (2013).
[6] G. S. Redner, M. F. Hagan, and A. Baskaran, Phys. Rev. Lett. **110**, 055701 (2013).
[7] Y. Fily and M. C. Marchetti, Phys. Rev. Lett. **108**, 235702 (2012).
[8] I. Buttinoni, J. Bialké, F. Kümmel, H. Löwen, C. Bechinger, and T. Speck, Phys. Rev. Lett. **110**, 238301 (2013).
[9] S. R. McCandlish, A. Baskaran, and M. F. Hagan, Soft Matter **8**, 2527 (2012).
[10] S. Ramaswamy, R. A. Simha, and J. Toner, Europhys. Lett. (EPL) **62**, 196 (2003).
[11] L. Giomi, T. B. Liverpool, and M. C. Marchetti, Phys. Rev. E **81**, 051908 (2010).
[12] D. Saintillan, Phys. Rev. E **81**, 056307 (2010).
[13] M. E. Cates, S. M. Fielding, D. Marenduzzo, E. Orlandini, and J. M. Yeomans, Phys. Rev. Lett. **101**, 068102 (2008).
[14] T. Shen and P. G. Wolynes, Proc. Nat. Acad. Sci. USA **101**, 8547 (2004).
[15] J. Bialké, T. Speck, and H. Löwen, Phys. Rev. Lett. **108**, 168301 (2012).
[16] J. Palacci, S. Sacanna, A. P. Steinberg, D. J. Pine, and P. M. Chaikin, Science **339**, 936 (2013).
[17] J. Palacci, C. Cottin-Bizonne, C. Ybert, and L. Bocquet, Phys. Rev. Lett. **105**, 088304 (2010).
[18] W. F. Paxton, K. C. Kistler, C. C. Olmeda, A. Sen, S. K. St. Angelo, Y. Cao, T. E. Mallouk, P. E. Lammert, and V. H. Crespi, J. Am. Chem. Soc. **126**, 13424 (2004).
[19] Y. Hong, N. M. K. Blackman, N. D. Kopp, A. Sen, and D. Velegol, Phys. Rev. Lett. **99**, 178103 (2007).
[20] S. Thutupalli, R. Seemann, and S. Herminghaus, New J. Phys. **13**, 073021 (2011).
[21] H.-R. Jiang, N. Yoshinaga, and M. Sano, Phys. Rev. Lett. **105**, 268302 (2010).
[22] G. Volpe, I. Buttinoni, D. Vogt, H.-J. Kümmerer, and C. Bechinger, Soft Matter **7**, 8810 (2011).
[23] V. Narayan, S. Ramaswamy, and N. Menon, Science **317**, 105 (2007).
[24] A. Kudrolli, G. Lumay, D. Volfson, and L. S. Tsimring, Phys. Rev. Lett. **100**, 058001 (2008).
[25] J. Deseigne, O. Dauchot, and H. Chaté, Phys. Rev. Lett. **105**, 098001 (2010).
[26] J. Schwarz-Linek, C. Valeriani, A. Cacciuto, M. E. Cates, D. Marenduzzo, A. N. Morozov, and W. C. K. Poon, Proc. Nat. Acad. Sci. USA **109**, 4052 (2012).
[27] I. Theurkauff, C. Cottin-Bizonne, J. Palacci, C. Ybert, and L. Bocquet, Phys. Rev. Lett. **108**, 268303 (2012).
[28] Neglecting hydrodynamic coupling can be justified by restricting the domain of applicability to motile cells on a surface [7], by noting that hydrodynamic coupling is screened and decays rapidly in space for particles close to a hard wall [29,30], or by observing as in two recent studies of active colloids [8,16] that the collective phenomena observed in experiments can be well reproduced in simulations without including hydrodynamic interactions.
[29] H. Diamant, B. Cui, B. Lin, and S. A. Rice, J. Phys. Condens. Matter **17**, S2787 (2005).
[30] E. R. Dufresne, T. M. Squires, M. P. Brenner, and D. G. Grier, Phys. Rev. Lett. **85**, 3317 (2000).
[31] A. C. Brańka and D. M. Heyes, Phys. Rev. E **60**, 2381 (1999).
[32] B. Smit and D. Frenkel, J. Chem. Phys. **94**, 5663 (1991).
[33] See Supplemental Material at http://link.aps.org/supplemental/10.1103/PhysRevE.88.012305 for movies of these systems.
[34] V. Trappe and P. Sandkühler, Curr. Opin. Colloid Interface Sci. **8**, 494 (2004).
[35] W. C. K. Poon, Curr. Opin. Colloid Interface Sci. **3**, 593 (1998).
[36] R. J. M. d'Arjuzon, W. Frith, and J. R. Melrose, Phys. Rev. E **67**, 061404 (2003).